



The year in cardiology 2017: imaging

Victoria Delgado¹, Juhani Knuuti², Sven Plein³, Stephan Achenbach⁴ and Jeroen J. Bax^{1*}

¹Department of Cardiology, Leiden University Medical Center, Albinusdreef 2, 2300 RC Leiden, The Netherlands; ²Turku PET Centre, University of Turku and Turku University Hospital, Kiinamyllynkatu 4-8, 20520 Turku, Finland; ³Multidisciplinary Cardiovascular Research Centre & Division of Biomedical Imaging, Leeds Institute of Cardiovascular and Metabolic Medicine, University of Leeds, Clarendon Wing, Leeds General Infirmary, Great George St, Leeds, LS1 3EX, UK; and ⁴Department of Cardiology, Friedrich-Alexander-Universität, Krankenhausstr. 12, 91054 Erlangen, Germany

Preamble

This Year in Cardiology 2017 review article provides a broad overview of the novelties published in non-invasive cardiovascular imaging. While it is well established that echocardiography is the imaging technique of first choice to evaluate patients with cardiovascular symptoms, other techniques (nuclear imaging, cardiovascular magnetic resonance, and computed tomography) are needed to image specific-disease characteristics or pathophysiological mechanisms that may impact on the patient's management. The evidence showing the incremental diagnostic and prognostic value of combination of imaging techniques or fusion imaging is growing exponentially. Advances in non-invasive cardiac imaging have provided important new insights in the pathophysiology of valvular heart disease and cardiomyopathies, risk stratification of patients with suspected coronary artery disease and diagnosis of implanted device- or bioprosthesis-related complications; this article provides an overview of the most relevant articles published in 2017.

Introduction

Advances in non-invasive cardiac imaging have provided important new insights in the pathophysiology of valvular heart disease and cardiomyopathies, risk stratification of patients with suspected coronary artery disease (CAD), and diagnosis of implanted device- or bioprosthesis-related complications. The evidence

showing the incremental diagnostic and prognostic value of combination of imaging techniques or fusion imaging is growing rapidly. This Year in Cardiology 2017 review article provides a broad overview of the novelties published in non-invasive cardiovascular imaging.

Echocardiography

The role of echocardiography in the diagnosis of valvular heart disease was underscored in the OxValve Population Cohort Study which recruited 2500 patients aged 65 years and older without known valvular heart disease (1). One in two of the elderly population had newly diagnosed (predominantly mild) valvular heart disease: 34% presented aortic sclerosis, 22% mitral regurgitation, and 15% aortic regurgitation. Moderate and severe undiagnosed valvular heart disease was identified in 6.4% of patients. Interestingly, moderate and severe valvular heart disease was three times more common in patients with atrial fibrillation (AF), which could be considered as a marker of silent significant valvular heart disease. Projections based on the OxValve Population Cohort Study suggest that the number of individuals aged 65 years or more in the UK will increase from 1.5 million in 2015 to 3 million by 2046. The results of this study provide further insights in the pathophysiology and natural history of valvular heart disease and have important implications for the management of elderly patients in the current era with growing advances in transcatheter therapies.

Selection of patients who may benefit from valvular intervention relies on symptoms and effects of the abnormal loading conditions on the cardiac chambers.

European Heart Journal 2018; 39, 275–285. doi:10.1093/eurheartj/ehx759

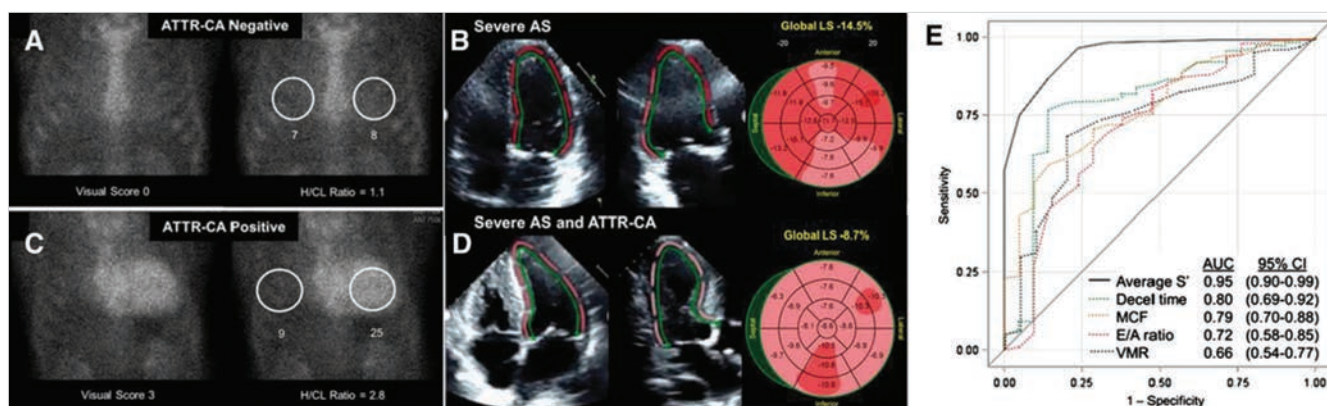
Received 7 November 2017; editorial decision 8 December 2017; accepted 9 December 2017; online publish-ahead-of-print 2 January 2018

The opinions expressed in this article are not necessarily those of the Editors of the European Heart Journal or of the European Society of Cardiology.

* Corresponding author. Tel.: +31 71 526 2020, Fax: +31 71 526 6809, Email: j.j.bax@lumc.nl

Published on behalf of the European Society of Cardiology. All rights reserved. © The Author(s) 2018.

For permissions, please email: journals.permissions@oup.com



This Figure has been reprinted by permission of Oxford University Press on behalf of the European Society of Cardiology

TAKE HOME FIGURE. Transthyretin cardiac amyloidosis in patients with severe aortic stenosis. Panels A and B show the technetium-99m pyrophosphate (^{99m}Tc-PYP) cardiac scintigraphy and the left ventricular global longitudinal strain bull's eye plot of a patient without transthyretin cardiac amyloidosis. A ^{99m}Tc-PYP cardiac scintigraphy positive for transthyretin cardiac amyloidosis shows an increased heart-to-contralateral ratio (H/CL) (panel C) and more impaired left ventricular global longitudinal strain (panel D). Panel E shows the receiver operating curves for several echocardiographic parameters of left ventricular systolic and diastolic dysfunction. The S' measured on tissue Doppler imaging had the largest area under the curve to predict ^{99m}Tc-PYP cardiac scintigraphy positive for transthyretin cardiac amyloidosis. Reproduced with permission from Castano et al. (3) AS, aortic stenosis; ATTR-CA, transthyretin cardiac amyloidosis; AUC, area under the curve; CI, confidence interval; Decel, deceleration; H/CL, heart-to-contralateral ratio; LS, longitudinal strain; MCF, myocardial contraction fraction; VMR, voltage-mass ratio

The extent of cardiac damage caused by the abnormal valve haemodynamics is an important determinant of the morbi-mortality of patients with heart valve disease. From the Placement of Aortic Transcatheter Valves (PARTNER)-2 trials, 1661 patients with severe stenosis were classified into four stages based on the cardiac damage assessed with echocardiography: no extra-valvular cardiac damage (Stage 0, n=47), left ventricular (LV) damage characterized by increased LV mass index (Stage 1, n=212), left atrial (LA), or mitral damage, including LA dilation, moderate, and severe mitral regurgitation and AF (Stage 2, n=814), pulmonary vasculature or tricuspid damage characterized by systolic pulmonary hypertension and moderate or severe tricuspid regurgitation (Stage 3, n=413) and right ventricular damage characterized by moderate and severe right ventricular dysfunction (Stage 4, n=145) (2). One-year mortality rates after aortic valve replacement increased along with progression of cardiac damage stage: from 4.4% in stage 0 to 24.5% in Stage 4. Each increment in cardiac damage stage was independently associated with increased mortality [hazard ratio (HR) 1.46, 95% confidence interval (CI) 1.27–1.67; P<0.0001].

Patients with symptomatic low-flow, low-gradient severe aortic stenosis may display significant cardiac damage with concentric LV hypertrophy and restrictive physiology, resembling cardiac amyloidosis. Between 6% and 12% of such patients may have transthyretin cardiac amyloidosis (3, 4). In 151 patients with severe aortic stenosis undergoing transcatheter aortic valve implantation, technetium-99m pyrophosphate (^{99m}Tc-PYP) cardiac scintigraphy was performed to evaluate the presence of concomitant transthyretin cardiac

amyloidosis and tissue Doppler echocardiography, as well as LV global longitudinal strain (GLS) with two-dimensional speckle tracking echocardiography to assess LV systolic function (5). Sixteen percent of patients had a ^{99m}Tc-PYP scan positive for transthyretin cardiac amyloidosis. Compared to patients with isolated severe aortic stenosis, patients with concomitant transthyretin cardiac amyloidosis showed more LV hypertrophy, lower stroke volume, more advanced LV diastolic dysfunction, and reduced LV function [lower LV ejection fraction (EF), more impaired LV GLS and lower peak systolic velocity on tissue Doppler imaging, S'] (*Take home figure*). A value of S' ≤6 cm/s on tissue Doppler echocardiography was strongly associated with a positive ^{99m}Tc-PYP scan. The clinical implications of these findings need to be evaluated in larger studies confirming that patients with concomitant transthyretin cardiac amyloidosis have worse prognosis after aortic valve replacement as compared to patients with isolated aortic stenosis.

The role of three-dimensional transoesophageal echocardiography to better characterize the mitral valve anatomy and dynamics in mitral regurgitation was highlighted in several publications. For example, *Kagiyama et al.* (6) demonstrated the presence of insufficient remodelling of the mitral leaflets assessed with three-dimensional transoesophageal echocardiography in 28 AF patients with moderate and severe mitral regurgitation compared to 56 AF patients without mitral regurgitation. The ratio between the total leaflet area and the mitral annulus area was significantly smaller among patients with moderate and severe mitral regurgitation than in patients without (1.29±0.10 vs. 1.65±0.24,

$P < 0.001$) indicating insufficient growth (remodelling) of the mitral leaflets to compensate for the dilation of the mitral annulus in AF (which then resulted in significant mitral regurgitation). Furthermore, *van Wijngaarden et al.* (7) demonstrated the different dynamics of the mitral valve annulus on three-dimensional transoesophageal echocardiography in patients with severe mitral regurgitation due to fibroelastic deficiency, Barlow's disease, and secondary mitral regurgitation. The mitral annulus dimensions were largest in patients with Barlow's disease whereas no differences were observed between patients with fibroelastic deficiency and patients with secondary mitral regurgitation. Along the cardiac cycle, the mitral annulus remained flat and less dynamic (the annulus height to the commissural width ratio was 18.24 ± 4.9 at early systole, 18.24 ± 4.7 at mid-systole, and 17.67 ± 4.4 at late systole, $P = 0.083$) in patients with secondary mitral regurgitation whereas patients with fibroelastic deficiency and Barlow's disease had more pronounced saddle-shaped mitral annulus which became significantly flatter at late systole (the annulus height to commissural width ratio changed from 21.99 ± 4.83 to 17.39 ± 4.2 in fibroelastic deficiency patients and from 23.89 ± 4.05 to 15.36 ± 4.2 in Barlow's disease patients; $P < 0.001$ for all). These findings suggest that mitral annulus mechanics are important pathophysiological determinants of the mitral valve dysfunction.

Standardization of novel echocardiographic techniques is key for implementation in routine clinical practice. Left ventricular GLS measurement has better inter-observer agreement than LVEF for follow-up of LV systolic function by multiple observers (8). In contrast, assessment of regional LV longitudinal strain has shown higher inter-vendor variability (9). Differences in image quality, tracking algorithms, and noise reduction by temporal and spatial smoothing across the various vendors may explain the high variability in regional strain measurements. Reproducible measurements of LV GLS and regional strain are important when echocardiographic follow-up is needed. In patients undergoing cancer treatment, early detection of cardiac dysfunction is the key to implement cardioprotective strategies to prevent irreversible cardiotoxicity. Left ventricular strain and strain rate measurements are more sensitive markers of LV systolic dysfunction than LVEF, which may enable earlier detection of cardiac damage. How these measures relate to ventricular-arterial coupling in this particular subgroup of patients was evaluated by Narayan et al (10). Of 135 patients with breast cancer receiving doxorubicin and trastuzumab, 15% developed cancer therapeutics-related cardiotoxicity over a median follow-up of 1.9 years. The ratio between effective arterial elastance and the end-systolic elastance (measure of ventricular-arterial coupling) and LV circumferential strain at baseline showed the largest area under the curve (AUC) to predict the occurrence of cancer therapeutics-related cardiotoxicity (0.703 and 0.655, respectively). However, these areas under the curve indi-

cate the modest discriminatory ability to identify the patients who will develop cardiotoxicity. Randomized clinical trials would be ideal to determine the external validity of these findings.

Nuclear imaging

Nuclear imaging provides unique, additional information to that provided by other imaging techniques. However, nuclear imaging involves ionizing radiation. In a recent consensus document by the three major European professional associations in the field of cardiac imaging, the best practices (technology, radiotracers, and data acquisition) to achieve the lowest radiation were summarized (11). In the field of nuclear cardiology, the use of new cadmium-zinc-telluride gamma cameras (that provide increased signal detection efficiency) and digital positron emission tomography (PET) detector technology based on silicon photomultipliers have resulted in a significant decrease in patient radiation burden (comparable to natural radiation exposure) without major impact on image quality and diagnostic accuracy.

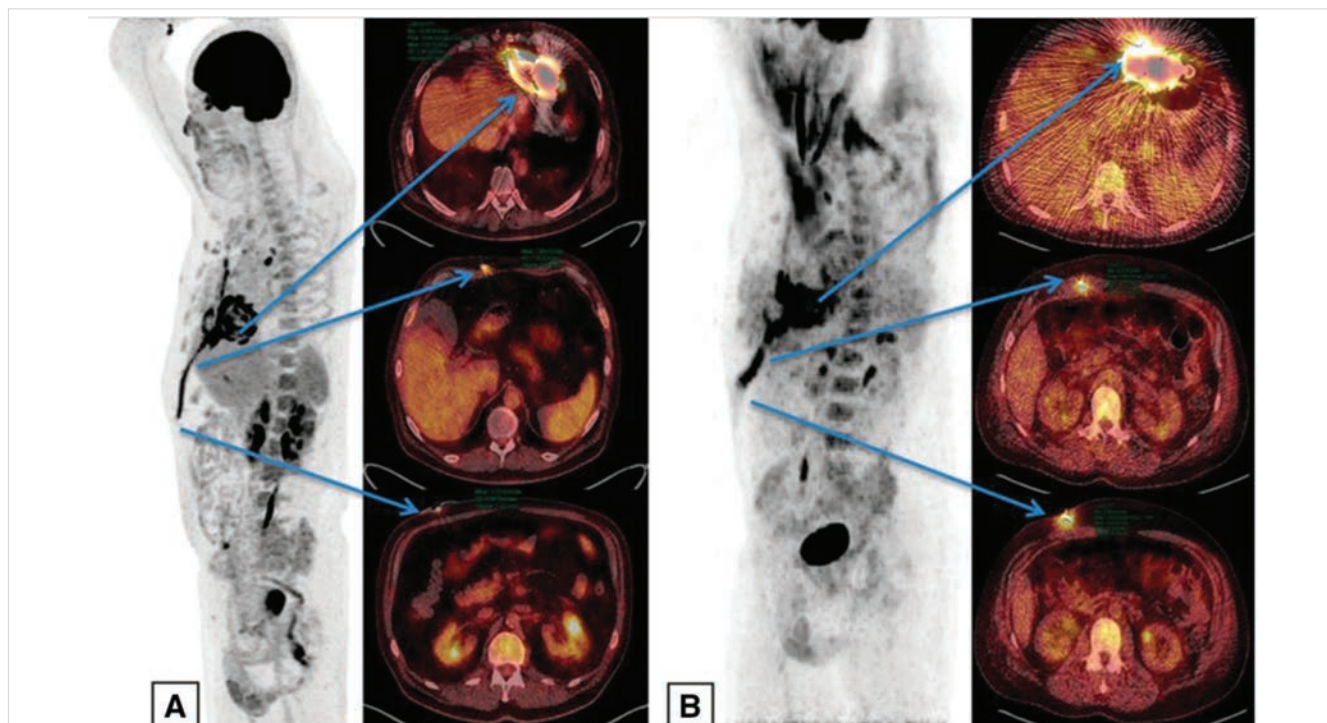
Both nuclear perfusion imaging and coronary computed tomography angiography (CCTA) provide important prognostic information. The association between atherosclerotic plaque features on CCTA and the presence of myocardial ischaemia on ^{99m}Tc -tetrofosmin stress/rest single photon emission computed tomography (SPECT) was evaluated in 184 patients with single vessel CAD (12). Total plaque volume and burden, and specifically for non-calcified, low-density non-calcified and calcified plaques, remodelling index, contrast density difference, lesion length, and diameter stenosis were significantly larger in those coronary arteries supplying ischaemic territories on myocardial perfusion imaging as compared with arteries supplying non-ischaemic territories. However, on multivariable analysis, non-calcified plaques (odds ratio 2.6), low-density non-calcified plaques (odds ratio 3.9) and contrast density difference (odds ratio 2.7) were significantly associated with ischaemia, whereas the degree of stenosis was not. The study demonstrated that other plaque characteristics than only coronary luminal narrowing are major determinants of myocardial ischaemia. These results provide interesting support for the concept that ischaemia reflects not only luminal narrowing but also relates to vulnerable plaques.

Cardiac sarcoidosis remains one of the major diagnostic challenges in cardiology. Cardiovascular magnetic resonance (CMR) and PET imaging are increasingly used to detect cardiac involvement of sarcoidosis. Imaging of active sarcoidosis with PET is based on detection of myocardial inflammation using ^{18}F -fluorodeoxyglucose (FDG). However, ^{18}F -FDG uptake is not specific for sarcoidosis. Although special patient preparation is applied to minimize myocardial glucose utilization, some degree of physiological ^{18}F -FDG uptake is commonly present in the heart. *Schildt et al.* (13) de-

monstrated the diagnostic accuracy of heterogeneity of myocardial ^{18}F -FDG uptake in 271 consecutive patients with suspected cardiac sarcoidosis referred for PET-computed tomography (CT). By quantifying the maximum, minimum, mean, and standard deviation of the segmental, ^{18}F -FDG uptake values of each of the 17 LV segments, the coefficient of variation of the entire left ventricle was calculated as the average of each segmental standard deviation divided by the average of each segmental mean. This coefficient of variation is a measure of LV metabolic heterogeneity. The investigators proposed a cut-off value of 0.184 to have the best accuracy to detect cardiac sarcoidosis (75% sensitivity, 51.4% specificity).

^{18}F -fluorodeoxyglucose PET has become one of the standard imaging tests in patients with suspected endocarditis (14). It has been shown earlier that PET provides important diagnostic information in patients with suspected prosthetic valve endocarditis. In contrast, the sensitivity of ^{18}F -FDG PET is low in native valve endocarditis if no annular involvement or extra-cardiac infection focus exist. In prosthetic valve endocarditis, relatively little information is available about the physiological ^{18}F -FDG uptake. *Mathieu et al* (15) characterized ^{18}F -FDG uptake patterns in non-infected prosthetic heart valves. The authors identified 54 prosthetic valves without endocarditis that have undergone ^{18}F -FDG PET imaging. Some degree of peri-prosthetic FDG uptake was present in

majority of prosthetic valves. The tracer uptake using quantitative analysis was significant in many patients and somewhat greater in mechanical than in biological valves (standardized uptake value 4.0 [2.4–8.0] and 3.3 [2.1–6.1], respectively). However, the pattern was typically homogeneous. Therefore, not only the intensity of ^{18}F -FDG uptake but also its heterogeneity is the important criteria for prosthetic valve endocarditis. Furthermore, *Dell'Aquila et al.* (16) demonstrated that quantitative ^{18}F -FDG PET-CT is an optimal diagnostic tool to detect superficial and deep driveline infections in heart failure patients recipients of continuous flow LV assist device. In contrast, the accuracy of quantitative ^{18}F -FDG PET-CT to diagnose pump housing infection is limited and a qualitative approach together with the clinical information should be considered in this situation (*Figure 1*). In addition, ^{18}F -FDG PET is increasingly used for the diagnosis of cardiac implantable electronic device infection. *Juneau et al.* (17) performed a systematic review and meta-analysis of the accuracy of PET and SPECT to detect cardiac implantable electronic device infection. A total of 13 articles (11 studies for ^{18}F -FDG PET-CT and 2 for labelled leucocyte scintigraphy) met the inclusion criteria. The pooled sensitivity of ^{18}F -FDG PET-CT for the diagnosis of cardiac implantable electronic device infection was 87% (95% CI 82%–91%) and pooled specificity was 94% (95% CI 88%–98%). The receiver operating characteristics curve analysis demonstrated good



This Figure has been reprinted by permission of Oxford University Press on behalf of the European Society of Cardiology

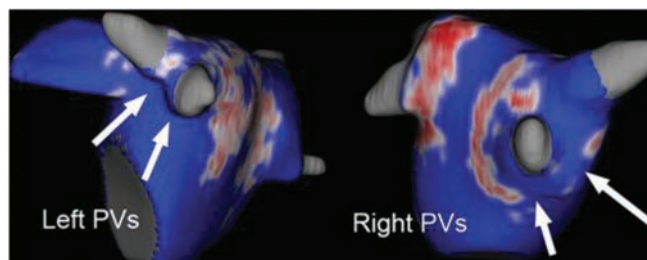
FIGURE 1. ^{18}F -fluorodeoxyglucose positron emission tomography–computed tomography to diagnose left ventricular assist device infection. On maximum intensity projections and fused transaxial positron emission tomography–computed tomography images, the pathological uptake of ^{18}F -fluorodeoxyglucose is visualized at the piercing site of the driveline and along the intracorporeal course in panel A whereas panel B shows pathological ^{18}F -fluorodeoxyglucose accumulation at all the levels including the pump housing. Reproduced with permission from Dell'Aquila et al (16)

accuracy overall, with an AUC of 0.935. For labelled leucocyte scintigraphy, both studies reported sensitivity above 90% and specificity of 100%. The authors concluded that both ^{18}F -FDG PET-CT and leucocyte scintigraphy yield high sensitivity, specificity, and accuracy, but limited data is available on the latter. The authors recommended to use ^{18}F -FDG PET as preferred method when available. Also leucocyte scintigraphy appears useful tool for the diagnosis of cardiac implantable electronic device infection.

Cardiovascular magnetic resonance

Among the established clinical applications of CMR, the measurement of cardiac iron loading has become an integral part of the management of patients with thalassaemia major and CMR guided management has dramatically reduced mortality in this patient population. In a recent cohort of 481 thalassaemia patients on contemporaneous treatment, *Pepe et al* (18) described which CMR findings are independently associated with the occurrence of heart failure and arrhythmias. Overall, the rate of adverse outcomes was low with only 16 patients experiencing heart failure and 16 presenting with an arrhythmia during 6 years follow-up. Myocardial fibrosis on late gadolinium enhancement (LGE) CMR was associated with adverse outcomes (HR=10.9, $P<0.001$), homogeneous myocardial iron overload (HR=5.6, $P=0.016$) and ventricular dysfunction (HR=4.33, $P=0.011$). Iron chelation management was changed in nearly 70% of patients as a result of the CMR study, underlining the clinical relevance of CMR in this condition.

The prognostic relevance of LGE CMR has also been the subject of several meta-analyses and single-centre studies in common and more rare diseases. *Raina et al.* (19) summarized the prognostic value of LGE from 7 studies with 425 systemic amyloidosis patients. Patients with evidence of fibrosis on LGE CMR had almost five times higher mortality at a mean follow-up of 25 months compared to those without LGE (pooled odds ratio: 4.96; 95% CI 1.90-12.93; $P=0.001$). In sarcoidosis, *Coleman et al.* (20) pooled the results of 10 studies with a total of 760 patients. The presence of LGE was associated with a three-fold increase in all-cause mortality at 3.0 ± 1.1 years and a 10-fold increase in a composite endpoint that also included ventricular arrhythmia, implantable cardioverter defibrillator shocks, and sudden cardiac death. In a large single-centre study, *Halliday et al.* (21) presented data on 399 patients with dilated cardiomyopathy and $\text{LVEF}\geq 40\%$. Patients underwent CMR including LGE and were followed-up for a median of 4.6 years. The presence of mid-wall fibrosis on LGE was associated with a 9.2-fold increase in the risk of a composite endpoint of sudden death and aborted sudden death, a five-fold increase in the risk of sudden cardiac death alone and a 35-fold increase in the risk of aborted sudden cardiac death. A small-

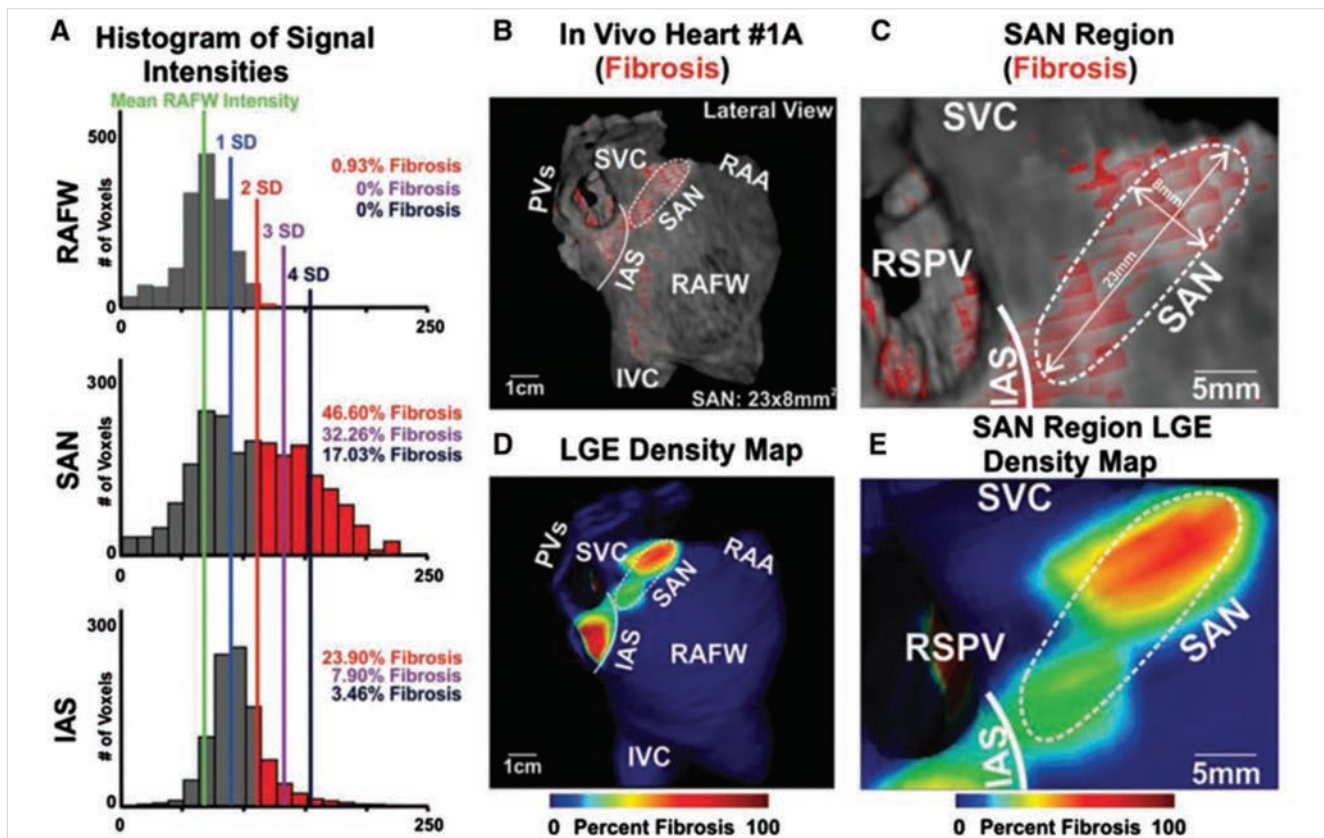


This Figure has been reprinted by permission of Oxford University Press on behalf of the European Society of Cardiology

FIGURE 2. Late gadolinium enhanced cardiovascular magnetic resonance images of the left atrium following pulmonary vein ablation for atrial fibrillation. The arrows point to gaps in the pulmonary vein encirclement. Reproduced with permission from *Gal and Marrouche*. (23) PV, pulmonary vein

ler single-centre study by *Pedrotti et al.* (22) examined the prognostic value of LGE in 48 patients with orthotopic heart transplantation. The strongest predictor of major adverse cardiovascular events was cardiac allograft vasculopathy (HR 3.63, $P=0.004$) followed by LGE mass (HR 1.04, $P=0.0007$) and percentage of LGE of LV mass (HR 1.083, $P=0.0002$). These meta-analyses and single-centre studies add to the expanding evidence supporting the use of LGE CMR as a strong marker of adverse clinical outcome in a wide range of diseases. The potential applications of LGE CMR in the management of AF were reviewed by *Gal and Marrouche*. (23) Late gadolinium enhancement CMR can be used to characterize LA fibrosis as a predictor of AF recurrence, as a guide to post-ablation success (*Figure 2*). Furthermore, *Csepe et al.* (24) reported that LGE can even be used to visualise the healthy human sinoatrial node, which consists of 35–55% fibrotic tissue surrounded by fatty tissue, providing mechanical and electrical protection from the surrounding atrial tissue. Using high-resolution 3T CMR, the sinoatrial node was visualized in four healthy volunteers and optically mapped with 9.4 T contrast-enhanced CMR in five explanted donor hearts (*Figure 3*). The CMR findings correlated closely with the findings from the histological sections. Combined with LGE of the LA, identification of the sinoatrial node location may further enhance the use of CMR in patients with AF and help to perform a more targeted ablation procedure.

While LGE is uniquely able to detect focal fibrosis and scar, T1 mapping CMR allows the detection and quantification of diffuse myocardial processes such as inflammation and fibrosis. *Liu et al.* (25) performed native T1 mapping as part of a comprehensive CMR protocol in 61 STEMI patients and showed that different thresholds of T1 values can differentiate between reversible and irreversible myocardial injury. The volume of myocardial damage using a native T1 threshold correlated with both troponin I release and 6 months of LVEF as a marker of LV remodelling. In a similar study design, *Garg et*

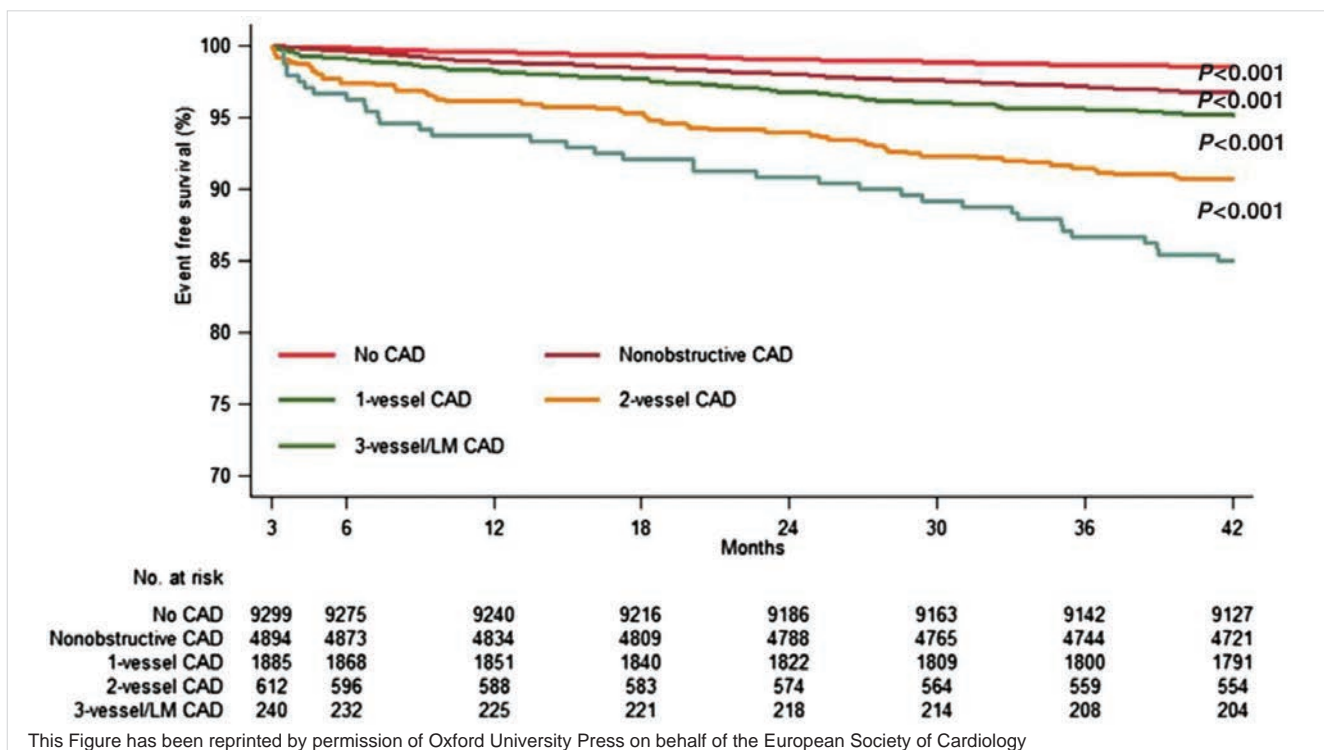


This Figure has been reprinted by permission of Oxford University Press on behalf of the European Society of Cardiology

FIGURE 3. Late gadolinium contrast enhanced cardiovascular magnetic resonance to identify the sinoatrial node. Panel A displays the histograms of total signal intensity of the right atrial free wall, sinoatrial node, and interatrial septum. To determine the percentage of fibrosis, the mean signal intensity of the right atrial free wall is considered the reference. Each standard deviation above the mean signal intensity of the right atrial free wall indicates increasing fibrosis. The lateral view of the three-dimensional reconstruction of the right atrium is presented in panel B. The red-shaded area indicates the sinoatrial node, demarcated by a white dashed line, and its dimensions are shown in a zoomed view in panel C. The density maps of the right atrium and the zoomed view of the sinoatrial node are displayed in panels D and E, respectively. Reproduced with permission from Csepe et al. (24) IAS, interatrial septum; IVC, inferior vena cava; PVs, pulmonary veins; RAA, right atrial appendage; RAFW, right atrial free wall; RSPV, right superior pulmonary vein; SAN, sinoatrial node; SVC, superior vena cava; SD, standard deviation.

al. (26) combined both native and post-contrast enhanced CMR to quantify the myocardial extracellular volume fraction in 50 patients who underwent CMR acutely (24–72h) after infarction and at 3 months of follow-up. Extracellular volume fraction acutely measured post-infarction correlated with the area at risk (assessed with T2-weighted CMR sequences) and final infarct size by LGE at 3 months. Finally, *Reinstadler et al.* (27) investigated native T1 in the non-infarcted remote zone in 225 ST-segment elevation myocardial infarction (STEMI) patients. Elevated native T1 values in the remote zone were noted in patients with larger infarcts, less myocardial salvage and worse LV function at baseline. In multivariable analysis, native T1 values of the remote zone were independently associated with major adverse cardiac events. Adding the native T1 values of the remote zone to other known prognostic CMR markers (LVEF, infarct size, and myocardial salvage index) led to a net reclassification improvement of 0.82 (95% CI 0.46–1.17; $P < 0.001$). These findings suggest that re-

mote zone characteristics in patients with STEMI may have clinical relevance and that native T1 mapping could be used to improve risk stratification. Multi-parametric CMR can characterize complex physiological processes in vivo. *Levelt et al.* (28) evaluated 31 patients with type 2 diabetes mellitus without CAD and 17 matched controls with adenosine stress CMR to derive a semi-quantitative myocardial perfusion reserve index, blood-oxygen level-dependent imaging, which measures myocardial oxygenation, and MR spectroscopy of the phosphocreatine to adenosine tri-phosphate (PCr/ATP) ratio to study myocardial energy handling. Data were acquired at rest and during exercise. At baseline, diabetic patients had a 17% lower PCr/ATP ratio compared with a control population, suggesting the presence of impaired energy handling, which worsened by 12% with exercise. In addition, during vasodilator stress, myocardial perfusion reserve index was 24% lower and oxygenation response was blunted in diabetic patients as compared to controls. These



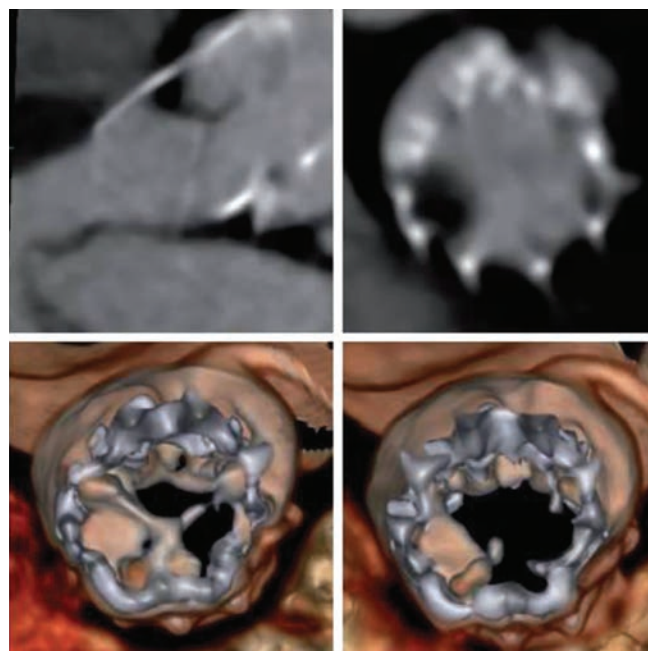
This Figure has been reprinted by permission of Oxford University Press on behalf of the European Society of Cardiology

FIGURE 4. Unadjusted event-free survival from the composite endpoint according to the extent of coronary artery disease. Composite endpoint comprising late coronary revascularization, myocardial infarction, and all-cause death. Reproduced with permission from Nielsen et al. (30) CAD, coronary artery disease.

observations support the concept that coronary microvascular dysfunction in diabetes exacerbates derangement of cardiac energetics under conditions of increased workload and underline the potential of quantitative multi-parametric CMR to study complex pathophysiological processes.

Computed tomography

Coronary calcium offers a possibility to detect and quantify subclinical atherosclerosis and identify individuals at increased risk for future cardiovascular events. In low-risk patients with chest pain and suspected CAD included in the Prospective Multicenter Imaging Study for Evaluation of Chest Pain (PROMISE) trial, Budoff et al. (29) analysed the prognostic value of coronary calcium. A total of 4602 patients who underwent coronary calcium imaging and CCTA were compared to a cohort of 4602 individuals who underwent functional ischaemia testing. Both cohorts were followed for 26 months and the occurrence of all-cause death, myocardial infarction, or unstable angina hospitalization was recorded. Overall, the ability to predict events was similar for coronary calcium and functional testing (C-statistic: 0.67 vs. 0.64)—with coronary calcium being more sensitive and functional testing being more specific. Interestingly, CCTA was significantly more predictive for events than both calcium and functional testing (C-statistic: 0.72). These results underscore the role of coronary calcium as marker of atherosclerosis burden and



This Figure has been reprinted by permission of Oxford University Press on behalf of the European Society of Cardiology

FIGURE 5. Portico valve with thick layer of hypo-attenuated leaflet thickening causing a severe reduction in leaflet motion (hypo-attenuation affecting motion). Top left panel: long axis multiplanar reconstruction in diastole; top right panel: axial multiplanar reconstruction diastole; Bottom left: diastolic volume rendering; bottom right: systolic volume rendering. Reproduced with permission from Sondergaard et al. (37)

predictor of cardiovascular events but quantification of coronary stenosis and plaque characterization with CCTA provide better discriminatory power to identify patients at risk.

The prognostic value of clinically indicated CCTA was evaluated in a large cohort by *Nielsen et al.* (30). In a region of Denmark, 16 949 patients older than 18 years who underwent CCTA for suspected CAD were systematically followed for the occurrence of a composite endpoint of late myocardial revascularization, myocardial infarction, and all-cause death during a 5 years' period. Revascularizations occurring within 90 days of CCTA were censored to exclude those that were triggered by the immediate CT findings. The composite endpoint occurred in 486 patients during a median follow-up period of 3.6 years. The risk of the composite endpoint was 1.5% for patients without identification of any coronary atherosclerosis on CCTA, 3.3% if non-obstructive plaque was present, and 6.8% for individuals with obstructive lesions in CCTA ($P < 0.001$ for all, *Figure 4*). If 3-vessel disease or left main stenosis was present, the risk was 15%. Interestingly, the predictive value of CCTA was maintained across all age groups, both in men and women.

The strong prognostic value of CCTA was also confirmed by *Deseive et al.* (31). Of 15 219 patients included in the international multicentre CONFIRM registry, 982 (6.5%) died during a median follow-up period of 5.3 years. The so-called CONFIRM score, (32) which combines the National Cholesterol Education Program Adult Treatment Panel (NCEP ATP) III score, the presence of proximal coronary artery segments containing plaque, and the presence of proximal coronary segments containing $>50\%$ stenoses, had superior prognostic value than clinical risk scores, including the NCEP ATP III, Framingham, and Morise scores (C-statistic: 0.696, 0.675, 0.610, and 0.606, respectively). Application of the CONFIRM score led to reclassification of 34% of patients when compared with the NCEP ATP III score alone.

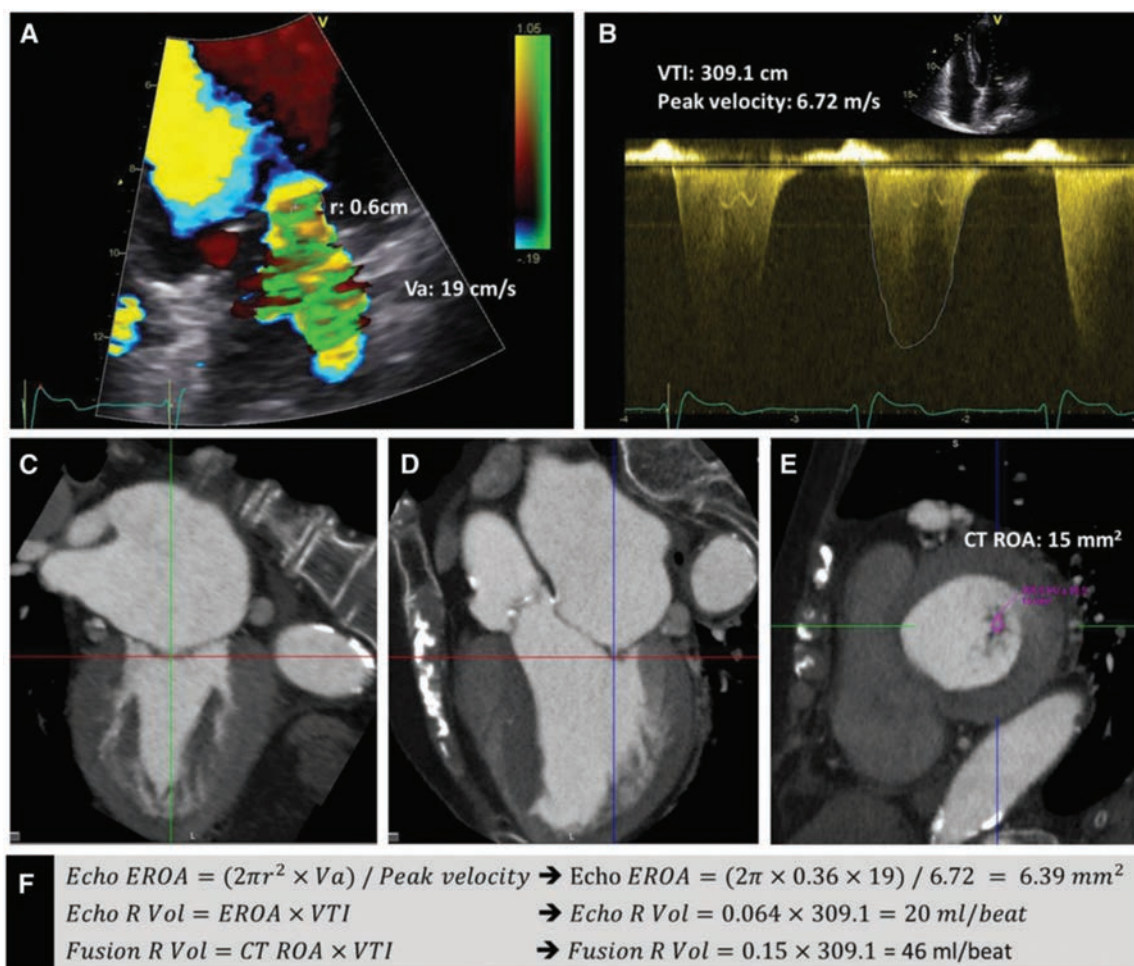
An interesting new approach to risk stratification based on CCTA was described by *Motwani et al.* (33) Machine learning was applied to build a model from clinical data and CCTA of 10 030 patients included in the CONFIRM registry. Twenty-five clinical variable (such as age, gender, and Framingham risk score) and 44 CCTA-derived parameters (such as segment stenosis score, segment involvement score, modified Duke index, number of segments with non-calcified, mixed or calcified plaques). Machine learning involved automated feature selection, model building, and 10-fold stratified cross-validation. During a mean follow-up of 5.4 years, 745 patients died. Machine learning yielded a higher AUC compared with the Framingham risk score or any single CCTA-derived severity scores alone (such as the segment involvement score) for predicting all-cause mortality (machine learning: 0.79; Framingham Risk Score: 0.61; seg-

ment involvement score: 0.64; $P < 0.001$). These results suggest that machine learning has an important role in correctly identifying the high-risk patients with suspected CAD who may benefit from intensified preventive treatment.

There are several approaches to add functional information (identification of ischaemia) to CCTA—which is an anatomic imaging technique. One approach is fractional flow reserve (FFR)-CT, the simulation of FFR based on CT-derived anatomic data sets. The other approach is myocardial CT perfusion during adenosine stress, which requires a separate CT acquisition. Both approaches are currently being validated. *Jensen et al.* (34) evaluated whether CCTA, combined with FFR-CT if deemed necessary, would allow to safely defer invasive coronary angiograms. Over a period of 6 months, 774 patients referred to invasive angiography or CCTA in a single centre were evaluated. Downstream testing, treatment within 3 months and adverse events were analysed. Patients were divided in two groups according to the presence of typical angina: low-intermediate-risk ($n=593$) and high-risk ($n=181$), with mean pre-test probabilities of CAD of $31 \pm 16\%$ and $67 \pm 16\%$, respectively. Coronary computed tomography angiography was supplemented by FFR-CT in 212 (28%) patients. In the high- and in the low-intermediate-risk group, invasive coronary angiography could be avoided in 75% and 91% of patients. Over a mean follow-up time of 157 ± 50 days, serious clinical events occurred in four patients. No events occurred in patients in whom invasive angiography had been cancelled due to inconspicuous findings in CCTA (with selective FFR-CT testing)—indicating that CCTA, in combination with FFR-CT when deemed necessary, allows to safely defer invasive angiography. In the FFR-CT (Does Routine Pressure Wire Assessment Influence Management Strategy at Coronary Angiography for Diagnosis of Chest Pain? (RIPCARD) study, (35) which analysed a cohort of 200 patients in a multicentre approach, FFR-CT led to a change of the downstream management plan after CCTA in 36% of patients.

The second approach, CT myocardial perfusion imaging, is also under clinical investigation. *Penagaluri et al.* (36) studied the diagnostic value of CT myocardial perfusion imaging in addition to CCTA in 381 patients. Patient-based diagnostic accuracy—defined by the area under the receiver operating curve—for CCTA alone was 0.83 and for CCTA-CT perfusion was 0.92 ($P=0.003$) in women. However, no significant difference was found in men (0.82 vs. 0.84, $P=0.29$). Future studies will be required to assess the optimal clinical utilization of CT myocardial perfusion imaging.

Cardiac CT imaging is not limited to the evaluation of CAD. Computed tomography plays an increasingly important role in the context of structural heart interventions, including transcatheter aortic valve implantation. A recent development has been the observation that both



This Figure has been reprinted by permission of Oxford University Press on behalf of the European Society of Cardiology

FIGURE 6. Integration of the Doppler echocardiography and computed tomography data to quantify mitral regurgitant volume. By echocardiography, the proximal isovelocity surface method was used for the assessment of the effective regurgitant orifice area of the mitral regurgitation. (Panels A, B, and F) The velocity time integral of the magnetic resonance jet was assessed on the continuous wave Doppler images (Panel B). By aligning the multiplanar reformation planes on the multi-detector computed tomography data, a double oblique transverse plane parallel to the narrowest part of the mitral regurgitant orifice was reconstructed. The anatomical mitral regurgitant orifice area was measured by planimetry at this level (Panels C–E). The echocardiography and integrated regurgitant volume of magnetic resonance were assessed by multiplying the echocardiographic effective regurgitant orifice area and the multi-detector computed tomography derived mitral regurgitant orifice area with the velocity time integral, respectively (Panel F). Reproduced with permission from van Rosendaal et al. (42) VTI, velocity time integral; CT, computed tomography; ROA, regurgitant orifice area; RVol, regurgitant volume; EROA, effective regurgitant orifice area.

transcatheter and surgically implanted aortic bioprosthetic valves may display ‘hypo-attenuated leaflet thickening’ (‘HALT’) (Figure 5) (37–40). The clinical significance of this observation, however, has been unclear: while in some studies the presence of HALT was not associated with increased risk of stroke, (37, 38) Chakravarty et al. (40) postulate a somewhat higher rate of cerebral ischemic events if HALT is present. Interestingly, the study by Sondergaard et al. (37) highlights the temporal evolution of HALT and demonstrates that HALT can progress to hypo-attenuation affecting motion (HAM) or regress and disappear. In 84 patients included in the Subclinical Aortic Valve Bioprosthesis Thrombosis Assessed With 4D CT (SAVORY) registry, two sequential CT scans were

performed at 140 and 298 days after valve implantation. Hypo-attenuated leaflet thickening and HAM were present in 38.1% and 20.2% of patients in the first scan and were highly dynamic, showing progression in 15.5% and regression in 10.7% of patients. Importantly, progression was less likely among patients treated with oral anticoagulation (OR 0.014, P=0.036), but regression could happen independently of the use of anticoagulants. The results of these studies have questioned current recommendations on the use of anticoagulation therapy for aortic bioprostheses. Additional studies using sequential imaging are needed to unravel the time-course of HALT and HAM and establish personalized anticoagulation treatment (41).

Hybrid imaging or fusion imaging

The literature reports an increasing use of fusion imaging in research but also in clinical cardiology. The different components of imaging can be categorized as anatomical, functional, and biological imaging. Coronary computed tomography angiography is a good example of anatomical imaging: visualizing the coronary arteries and potential stenoses; echocardiography and CMR provide both functional and anatomical imaging. Nuclear imaging can offer functional imaging (ischaemia assessment) but is currently the only technique that provides biological imaging: e.g. inflammation assessment with ^{18}F -FDG. Fusion imaging could represent the fusion or integration of different images that were acquired in isolation and then later on fused or integrated for assessment of cardiovascular pathophysiology. For example, *van Rosendaal et al.* (42) described the integrated use of CT and echocardiography for improved assessment of severity of mitral regurgitation in 73 patients. When the effective regurgitant orifice was assessed by direct planimetry from CT, and this orifice size was then integrated with the velocity of the regurgitant flow on echocardiography (*Figure 6*), the severity of mitral regurgitation was downgraded from severe to non-severe in 10% of patients and upgraded from non-severe to severe in 14% of patients. Thus the fusion of the two techniques altered severity assessment in 24% of patients; the prognostic value of this fusion imaging remains to be demonstrated.

The majority of the literature reports on hybrid imaging, mostly with PET and CT, but also with PET and CMR. These new machines permit direct fusion of both images, which are acquired simultaneously or sequentially (in the same session). Various examples were reported in 2017. *Singh et al.* (43) reported on integrated imaging of coronary plaque morphology and inflammation using PET-CT with ^{18}F -FDG: 55 patients underwent imaging before and after 12 weeks of statin (atorvastatin) use. The ^{18}F -FDG uptake (target-to-background ratio) was assessed in the left main coronary artery, which was significantly higher in non-calcified or partially calcified lesions on CCTA (considered high-risk) as com-

pared to calcified lesions (target-to-background ratios 1.95 ± 0.43 vs. 1.67 ± 0.32 , $P=0.04$). After 12 weeks of statin use, there was a significant reduction in ^{18}F -FDG uptake in the high-risk lesions.

Patients ($n=25$) with possible sarcoidosis were evaluated with PET-CMR; (44) active sarcoidosis was defined as having increased ^{18}F -FDG uptake in areas with delayed contrast-enhancement on CMR (present in eight patients); all other patients did not show active sarcoidosis. This approach may enable identification of patients with active sarcoidosis and permit selective treatment.

Positron emission tomography–computed tomography enabled accurate detection of endocarditis in patients who underwent transcatheter aortic valve replacement (45). Computed tomography demonstrated leaflet thickening (as marker of thrombosis), whereas ^{18}F -FDG indicated active inflammation; the imaging approach was superior over routine assessment of endocarditis (according to the modified Duke criteria).

In the EVAluation of INtegrated Cardiac Imaging for the Detection and Characterization of Ischaemic Heart Disease (EVINCI) study, 14 centres from nine European countries included 252 patients with stable angina and intermediate pre-test likelihood of CAD (46). The patients underwent SPECT or PET perfusion imaging and CCTA, and these images were fused on a dedicated workstation. These non-invasive imaging data were compared with quantitative invasive coronary angiography with assessment of FFR (to detect haemodynamically significant stenosis). Hybrid imaging excluded functionally significant CAD in 41% of patients, which provided a negative predictive value of 88%, and included in significant disease in 24% of patients, which yielded a positive predictive value of 87%. To establish the role of hybrid imaging in the detection of significant CAD, additional studies are needed focusing on the influence of this imaging modality on the downstream of patients (avoiding unnecessary invasive coronary angiography and interventions).

Conflict of interest: none declared.

Copyright: [European Heart Journal 2018; 39 (4): 275–285]

Published on behalf of the European Society of Cardiology. All rights reserved. © The Author(s) 2018. For permissions please email: journals.permissions@oup.com

Drug and Material Disclaimer:

The mention of trade names, commercial products organizations, and the inclusion of advertisements in the journal does not imply endorsement by the European Heart journal, the editors, the editorial board, Oxford University Press or the organization to which the authors are affiliated. The editors and publishers have taken all reasonable precautions to verify drug names and doses, the results of experimental work and clinical findings published in the journal. The ultimate responsibility for the use and dosage of drugs mentioned in the journal and in interpretation of published material lies with the medical practitioner, and the editors and publisher cannot accept liability for damages arising from any error or omissions in the journal. Please inform the editors of any errors.

The opinions expressed in the European Heart Journal are those of the authors and contributors, and do not necessarily reflect those of the European Society of Cardiology, the editors, the editorial board, Oxford University Press or the organization to which the authors are affiliated.

References

1. d'Arcy JL, Coffey S, Loudon MA, Kennedy A, Pearson-Stuttard J, Birks J, Frangou E, Farmer AJ, Mant D, Wilson J, Myerson SG, Prendergast BD. Large-scale community echocardiographic screening reveals a major burden of undiagnosed valvular heart disease in older people: the OxVALVE Population Cohort Study. *Eur Heart J* 2016;37:3515–3522.
2. Genereux P, Pibarot P, Redfors B, Mack MJ, Makkar RR, Jaber WA, Svensson LG, Kapadia S, Tuzcu EM, Thourani VH, Babaliaros V, Herrmann HC, Szeto WY, Cohen DJ, Lindman BR, McAndrew T, Alu MC, Douglas PS, Hahn RT, Kodali SK, Smith CR, Miller DC, Webb JG, Leon MB. Staging classification of aortic stenosis based on the extent of cardiac damage. *Eur Heart J* 2017;38:3351–3358.
3. Castano A, Narotsky DL, Hamid N, Khaliq OK, Morgenstern R, DeLuca A, Rubin J, Chiuzan C, Nazif T, Vahl T, George I, Kodali S, Leon MB, Hahn R, Bokhari S, Maurer MS. Unveiling transthyretin cardiac amyloidosis and its predictors among elderly patients with severe aortic stenosis undergoing transcatheter aortic valve replacement. *Eur Heart J* 2017;38:2879–2887.
4. Treibel TA, Fontana M, Gilbertson JA, Castelletti S, White SK, Scully PR, Roberts N, Hutt DF, Rowczenio DM, Whelan CJ, Ashworth MA, Gillmore JD, Hawkins PN, Moon JC. Occult transthyretin cardiac amyloid in severe calcific aortic stenosis: prevalence and prognosis in patients undergoing surgical aortic valve replacement. *Circ Cardiovasc Imaging* 2016;9:e005066.
5. Longhi S, Lorenzini M, Gagliardi C, Milandri A, Marzocchi A, Marzocchini C, Saia F, Ortolani P, Biagini E, Guidalotti PL, Leone O, Rapezzi C. Coexistence of degenerative aortic stenosis and wild-type transthyretin-related cardiac amyloidosis. *JACC Cardiovasc Imaging* 2016;9:325–327.
6. Kagiya N, Hayashida A, Toki M, Fukuda S, Ohara M, Hirohata A, Yamamoto K, Isobe M, Yoshida K. Insufficient leaflet remodeling in patients with atrial fibrillation: association with the severity of mitral regurgitation. *Circ Cardiovasc Imaging* 2017;10:e005451.
7. van Wijngaarden SE, Kamperidis V, Regeer MV, Palmen M, Schalijs MJ, Klautz RJ, Bax JJ, Ajmone MN, Delgado V. Three-dimensional assessment of mitral valve annulus dynamics and impact on quantification of mitral regurgitation. *Eur Heart J Cardiovasc Imaging* 2017. doi:10.1093/ehjci/jex001.
8. Negishi T, Negishi K, Thavendiranathan P, Cho GY, Popescu BA, Vinereanu D, Kurosawa K, Penicka M, Marwick TH. Effect of experience and training on the concordance and precision of strain measurements. *JACC Cardiovasc Imaging* 2017;10:518–522.
9. Mirea O, Pagourelas ED, Duchenne J, Bogaert J, Thomas JD, Badano LP, Voigt JU. Variability and reproducibility of segmental longitudinal strain measurement: a report from the EACVI-ASE strain standardization task force. *JACC Cardiovasc Imaging* 2017. doi:10.1016/j.jcmg.2017.01.027.
10. Narayan HK, French B, Khan AM, Plappert T, Hyman D, Bajulaiye A, Domchek S, DeMichele A, Clark A, Matro J, Bradbury A, Fox K, Carver JR, Ky B. Noninvasive measures of ventricular-arterial coupling and circumferential strain predict cancer therapeutics-related cardiac dysfunction. *JACC Cardiovasc Imaging* 2016;9:1131–1141.
11. Gimelli A, Achenbach S, Buechel RR, Edvardsen T, Franccone M, Gaemperli O, Hacker M, Hyafil F, Kaufmann PA, Lancellotti P, Nieman K, Pontone G, Pugliese F, Verberne HJ, Gutberlet M, Bax JJ, Neglia D. Strategies for radiation dose reduction in nuclear cardiology and cardiac computed tomography imaging: a report from the European Association of Cardiovascular Imaging (EACVI), the Cardiovascular Committee of European Association of Nuclear Medicine (EANM), and the European Society of Cardiovascular Radiology (ESCR). *Eur Heart J* 2018;39:286–294.
12. Diaz-Zamudio M, Fuchs TA, Slomka P, Otaki Y, Arsanjani R, Gransar H, Germano G, Berman DS, Kaufmann PA, Dey D. Quantitative plaque features from coronary computed tomography angiography to identify regional ischemia by myocardial perfusion imaging. *Eur Heart J Cardiovasc Imaging* 2017;18:499–507.
13. Schildt JV, Loimaala AJ, Hippelainen ET, Ahonen AA. Heterogeneity of myocardial 2-[18F]fluoro-2-deoxy-D-glucose uptake is a typical feature in cardiac sarcoidosis: a study of 231 patients. *Eur Heart J Cardiovasc Imaging* 2017. doi:10.1093/ehjci/jex175.
14. Habib G, Lancellotti P, Antunes MJ, Bongiorni MG, Casalta JP, Del ZF, Dulgheru R, El KG, Erba PA, Iung B, Miro JM, Mulder BJ, Plonska-Gosciniak E, Price S, Roos-Hesselink J, Snygg-Martyn U, Thuny F, Tornos MP, Vilacosta I, Zamorano JL, Erol C, Nihoyanopoulos P, Aboyans V, Agewall S, Athanassopoulos G, Aytekin S, Benzer W, Bueno H, Broekhuizen L, Carerj S, Cosyns B, De BJ, De BM, Dimopoulos K, Donal E, Drexel H, Flachskampf FA, Hall R, Halvorsen S, Hoen B, Kirchhof P, Lainscak M, Leite MAF, Lip GY, Mestres CA, Piepoli MF, Punjabi PP, Rapezzi C, Rosenhek R, Siebens K, Tamargo J, Walker DM. 2015 ESC guidelines for the management of infective endocarditis: the task force for the management of infective endocarditis of the European Society of Cardiology (ESC). Endorsed by: European Association for Cardio-Thoracic Surgery (EACTS), the European Association of Nuclear Medicine (EANM). *Eur Heart J* 2015;36:3075–3128.
15. Mathieu C, Mikail N, Benali K, Iung B, Duval X, Nataf P, Jondeau G, Hyafil F, Le GD, Rouzet F. Characterization of 18F-fluorodeoxyglucose uptake pattern in noninfected prosthetic heart valves. *Circ Cardiovasc Imaging* 2017;10:e005585.
16. Dell'Aquila AM, Avramovic N, Mastrobuoni S, Motekallemi A, Wisniewski K, Scherer M, Sindermann JR, Wenning C. Fluorine-18 fluorodeoxyglucose positron emission tomography/computed tomography for improving diagnosis of infection in patients on CF-LVAD: longing for more 'insights'. *Eur Heart J Cardiovasc Imaging* 2017. doi:10.1093/ehjci/jex158.
17. Juneau D, Golfam M, Hazra S, Zuckier LS, Garas S, Redpath C, Bernick J, Leung E, Chih S, Wells G, Beanlands RS, Chow BJ. Positron emission tomography and single-photon emission computed tomography imaging in the diagnosis of cardiac implantable electronic device infection: a systematic review and meta-analysis. *Circ Cardiovasc Imaging* 2017;10:e005772.
18. Pepe A, Meloni A, Rossi G, Midiri M, Missere M, Valeri G, Sorrentino F, D'Ascola DG, Spasiano A, Filosa A, Cuccia L, Dello IN, Forni G, Caruso V, Maggio A, Pitrolo L, Peluso A, De MD, Positano V, Wood JC. Prediction of cardiac complications for thalassemia major in the widespread cardiac magnetic resonance era: a prospective multicentre study by a multi-parametric approach. *Eur Heart J Cardiovasc Imaging* 2017. doi:10.1093/ehjci/jex012.
19. Raina S, Lensing SY, Nairouz RS, Pothineni NV, Hakeem A, Bhatti S, Pandey T. Prognostic value of late gadolinium enhancement CMR in systemic amyloidosis. *JACC Cardiovasc Imaging* 2016;9:1267–1277.
20. Coleman GC, Shaw PW, Balfour PC Jr, Gonzalez JA, Kramer CM, Patel AR, Salerno M. Prognostic value of myocardial scarring on CMR in patients with cardiac sarcoidosis. *JACC Cardiovasc Imaging* 2017;10:411–420.
21. Halliday BP, Gulati A, Ali A, Guha K, Newsome S, Arzanauskaitė M, Vassiliou VS, Lota A, Izgi C, Tayal U, Khaliq Z, Stirrat C, Auger D, Pareek N, Ismail TF, Rosen SD, Vazir A, Alpendurada F, Gregson J, Frenneaux MP, Cowie MR, Cleland JGF, Cook SA, Pennell DJ, Prasad SK. Association between midwall late gadolinium enhancement and sudden cardiac death in patients with dilated cardiomyopathy and mild and moderate left ventricular systolic dysfunction. *Circulation* 2017;135:2106–2115.
22. Pedrotti P, Vittori C, Facchetti R, Pedretti S, Dellegrattaglia S, Milazzo A, Frigerio M, Cipriani M, Giannattasio C, Roghi A, Rimoldi O. Prognostic impact of late gadolinium enhancement in the risk stratification of heart transplant patients. *Eur Heart J Cardiovasc Imaging* 2017;18:130–137.
23. Gal P, Marrouche NF. Magnetic resonance imaging of atrial fibrosis: redefining atrial fibrillation to a syndrome. *Eur Heart J* 2017;38:14–19.
24. Csepe TA, Zhao J, Sul LV, Wang Y, Hansen BJ, Li N, Ignozzi AJ, Bratasz A, Powell KA, Kilic A, Mohler PJ, Janssen PML, Hummel JD, Simonetti OP, Fedorov VV. Novel application of 3D contrast-enhanced CMR to define fibrotic structure of the human sinoatrial node in vivo. *Eur Heart J Cardiovasc Imaging* 2017;18:862–869.
25. Liu D, Borlotti A, Viliani D, Jerosch-Herold M, Alkhalil M, De Maria GL, Fahrni G, Dawkins S, Wijesurendra R, Francis J, Ferreira V, Piechnik S, Robson MD, Banning A, Choudhury R, Neubauer S, Channon K, Kharbada R, Dall'armellina E. CMR native T1 mapping allows differentiation of reversible versus irreversible myocardial damage in ST-segment-elevation myocardial infarction: an OxAMI

- study (Oxford acute myocardial infarction). *Circ Cardiovasc Imaging* 2017;10:e005986.
- 26.** Garg P, Broadbent DA, Swoboda PP, Foley JRJ, Fent GJ, Musa TA, Ripley DP, Erhayiem B, Dobson LE, McDiarmid AK, Haaf P, Kidambi A, van der Geest RJ, Greenwood JP, Plein S. Acute infarct extracellular volume mapping to quantify myocardial area at risk and chronic infarct size on cardiovascular magnetic resonance imaging. *Circ Cardiovasc Imaging* 2017;10:e006182.
- 27.** Reinstadler SJ, Stiermaier T, Liebetrau J, Fuernau G, Eitel C, de WS, Desch S, Reil JC, Poss J, Metzler B, Lucke C, Gutberlet M, Schuler G, Thiele H, Eitel I. Prognostic significance of remote myocardium alterations assessed by quantitative noncontrast T1 mapping in ST-segment elevation myocardial infarction. *JACC Cardiovasc Imaging* 2017. doi:10.1016/j.jcmg.2017.03.015.
- 28.** Levelt E, Rodgers CT, Clarke WT, Mahmod M, Ariga R, Francis JM, Liu A, Wijesurendra RS, Dass S, Sabharwal N, Robson MD, Holloway CJ, Rider OJ, Clarke K, Karamitsos TD, Neubauer S. Cardiac energetics, oxygenation, and perfusion during increased workload in patients with type 2 diabetes mellitus. *Eur Heart J* 2016;37:3461–3469.
- 29.** Budoff MJ, Mayrhofer T, Ferencik M, Bittner DO, Lee KL, Lu MT, Coles A, Jang JJ, Krishnam MS, Douglas PS, Hoffmann U. The prognostic value of coronary artery calcium in the PROMISE study. *Circulation* 2017;36:1993–2005.
- 30.** Nielsen LH, Botker HE, Sorensen HT, Schmidt M, Pedersen L, Sand NP, Jensen JM, Steffensen FH, Tilsted HH, Botcher M, Diederichsen A, Lambrechtsen J, Kristensen LD, Ovrehus KA, Mickley H, Munkholm H, Gotzsche O, Husain M, Knudsen LL, Norgaard BL. Prognostic assessment of stable coronary artery disease as determined by coronary computed tomography angiography: a Danish multicentre cohort study. *Eur Heart J* 2017;38:413–421.
- 31.** Deseive S, Shaw LJ, Min JK, Achenbach S, Andreini D, Al-Mallah MH, Berman DS, Budoff MJ, Callister TQ, Cademartiri F, Chang HJ, Chinnaiyan K, Chow BJ, Cury RC, DeLago A, Dunning AM, Feuchtner G, Kaufmann PA, Kim YJ, Leipsic J, Marques H, Maffei E, Pontone G, Raff G, Rubinshtein R, Villines TC, Hausleiter J, Hadamitzky M. Improved 5-year prediction of all-cause mortality by coronary CT angiography applying the CONFIRM score. *Eur Heart J Cardiovasc Imaging* 2017;18:286–293.
- 32.** Hadamitzky M, Achenbach S, Al-Mallah M, Berman D, Budoff M, Cademartiri F, Callister T, Chang HJ, Cheng V, Chinnaiyan K, Chow BJ, Cury R, DeLago A, Dunning A, Feuchtner G, Gomez M, Kaufmann P, Kim YJ, Leipsic J, Lin FY, Maffei E, Min JK, Raff G, Shaw LJ, Villines TC, Hausleiter J. Optimized prognostic score for coronary computed tomographic angiography: results from the CONFIRM registry (COronary CT Angiography Evaluation For Clinical Outcomes: an InteRnational Multicenter Registry). *J Am Coll Cardiol* 2013;62:468–476.
- 33.** Motwani M, Dey D, Berman DS, Germano G, Achenbach S, Al-Mallah MH, Andreini D, Budoff MJ, Cademartiri F, Callister TQ, Chang HJ, Chinnaiyan K, Chow BJ, Cury RC, DeLago A, Gomez M, Gransar H, Hadamitzky M, Hausleiter J, Hindoyan N, Feuchtner G, Kaufmann PA, Kim YJ, Leipsic J, Lin FY, Maffei E, Marques H, Pontone G, Raff G, Rubinshtein R, Shaw LJ, Stehli J, Villines TC, Dunning A, Min JK, Slomka PJ. Machine learning for prediction of all-cause mortality in patients with suspected coronary artery disease: a 5-year multicentre prospective registry analysis. *Eur Heart J* 2017;38:500–507.
- 34.** Jensen JM, Botker HE, Mathiassen ON, Grove EL, Ovrehus KA, Pedersen KB, Terkelsen CJ, Christiansen EH, Maeng M, Leipsic J, Kaltoft A, Jakobsen L, Sorensen JT, Thim T, Kristensen S, Krusell LR, Norgaard BL. Computed tomography derived fractional flow reserve testing in stable patients with typical angina pectoris: influence on downstream rate of invasive coronary angiography. *Eur Heart J Cardiovasc Imaging* 2017. doi:10.1093/ehjci/jex068.
- 35.** Curzen NP, Nolan J, Zaman AG, Norgaard BL, Rajani R. Does the routine availability of CT-derived FFR influence management of patients with stable chest pain compared to CT angiography alone? The FFRCT RIPCORDER study. *JACC Cardiovasc Imaging* 2016;9:1188–1194.
- 36.** Penagaluri A, Higgins AY, Vavere AL, Miller JM, Arbab-Zadeh A, Betoko A, Steveson C, Zimmermann E, Cox C, Rochitte CE, Dewey M, Kofoed KF, Niinuma H, Di Carli MF, Lima JA, Chen MY. Computed tomographic perfusion improves diagnostic power of coronary computed tomographic angiography in women: analysis of the CORE320 trial (coronary artery evaluation using 320-row multi-detector computed tomography angiography and myocardial perfusion) according to gender. *Circ Cardiovasc Imaging* 2016;9:e005189.
- 37.** Sondergaard L, De BO, Kofoed KF, Jilaihawi H, Fuchs A, Chakravarty T, Kashif M, Kazuno Y, Kawamori H, Maeno Y, Bieliauskas G, Guo H, Stone GW, Makkar R. Natural history of subclinical leaflet thrombosis affecting motion in bioprosthetic aortic valves. *Eur Heart J* 2017;38:2201–2207.
- 38.** Vollema EM, Kong WKF, Katsanos S, Kamperidis V, van Rosendaal PJ, van der Kley F, de WA, Ajmone MN, Delgado V, Bax JJ. Transcatheter aortic valve thrombosis: the relation between hypo-attenuated leaflet thickening, abnormal valve haemodynamics, and stroke. *Eur Heart J* 2017;38:1207–1217.
- 39.** Jose J, Sulimov DS, El-Mawardi M, Sato T, Allali A, Holy EW, Becker B, Landt M, Kebernik J, Schwarz B, Richardt G, Abdel-Wahab M. Clinical bioprosthetic heart valve thrombosis after transcatheter aortic valve replacement: incidence, characteristics, and treatment outcomes. *JACC Cardiovasc Interv* 2017;10:686–697.
- 40.** Chakravarty T, Søndergaard L, Friedman J, De Backer O, Berman D, Kofoed KF, Jilaihawi H, Shiota T, Abramowitz Y, Jørgensen TH, Rami T, Israr S, Fontana G, de Knecht M, Fuchs A, Lyden P, Trento A, Bhatt DL, Leon MB, Makkar RR, Ramzy D, Cheng W, Siegel RJ, Thomson LM, Mangat G, Hariri B, Sawaya FJ, Iversen HK. Subclinical leaflet thrombosis in surgical and transcatheter bioprosthetic aortic valves: an observational study. *Lancet* 2017;389:2383–2392.
- 41.** Bax JJ, Delgado V. Further insight into transcatheter and surgical aortic bioprosthetic valve thrombosis. *Eur Heart J* 2017;38:2208–2210.
- 42.** van Rosendaal PJ, van Wijngaarden SE, Kamperidis V, Kong WKF, Leung M, Ajmone MN, Delgado V, Bax JJ. Integrated imaging of echocardiography and computed tomography to grade mitral regurgitation severity in patients undergoing transcatheter aortic valve implantation. *Eur Heart J* 2017;38:2221–2226.
- 43.** Singh P, Emami H, Subramanian S, Maurovich-Horvat P, Marincheva-Savcheva G, Medina HM, Abdelbaky A, Alon A, Shankar SS, Rudd JH, Fayad ZA, Hoffmann U, Tawakol A. Coronary plaque morphology and the anti-inflammatory impact of atorvastatin: a multicenter 18F-Fluorodeoxyglucose positron emission tomographic/computed tomographic study. *Circ Cardiovasc Imaging* 2016;9:e004195.
- 44.** Dweck MR, Abgral R, Trivieri MG, Robson PM, Karakatsanis N, Mani V, Palmisano A, Miller MA, Lala A, Chang HL, Sanz J, Contreras J, Narula J, Fuster V, Padilla M, Fayad ZA, Kovacic JC. Hybrid magnetic resonance imaging and positron emission tomography with fluorodeoxyglucose to diagnose active cardiac sarcoidosis. *JACC Cardiovasc Imaging* 2017. doi:10.1016/j.jcmg.2017.02.021.
- 45.** Salaun E, Sportouch L, Barral PA, Hubert S, Lavoute C, Casalta AC, Pradier J, Ouk D, Casalta JP, Lambert M, Gouriet F, Gaubert JY, Dehaene A, Jacquier A, Tessonnier L, Haentjens J, Theron A, Riberi A, Cammilleri S, Grisoli D, Jaussaud N, Collart F, Bonnet JL, Camoin L, Renard S, Cuisset T, Avierinos JF, Lepidi H, Mundler O, Raoult D, Habib G. Diagnosis of infective endocarditis after TAVR: value of a multimodality imaging approach. *JACC Cardiovasc Imaging* 2017. doi:10.1016/j.jcmg.2017.05.016.
- 46.** Liga R, Vontobel J, Rovai D, Marinelli M, Caselli C, Pietila M, Teresinska A, Aguade-Bruix S, Pizzi MN, Todiere G, Gimelli A, Chiappino D, Marraccini P, Schroeder S, Drosch T, Poddighe R, Casolo G, Anagnostopoulos C, Pugliese F, Rouzet F, Le GD, Cappelli F, Valente S, Gensini GF, Zawaideh C, Capitanio S, Sambucetti G, Marsico F, Filardi PP, Fernandez-Golfín C, Rincon LM, Graner FP, de Graaf MA, Stehli J, Reyes E, Nkomo S, Maki M, Lorenzoni V, Turchetti G, Carpeggiani C, Puzzuoli S, Mangione M, Marchesni P, Giannetti D, Nekolla S, Lombardi M, Sicari R, Scholte AJ, Zamorano JL, Underwood SR, Knuuti J, Kaufmann PA, Neglia D, Gaemperli O. Multicentre multi-device hybrid imaging study of coronary artery disease: results from the evaluation of integrated cardiac imaging for the detection and characterization of ischaemic heart disease (EVINCI) hybrid imaging population. *Eur Heart J Cardiovasc Imaging* 2016;17:951–960.